AGU PUBLICATIONS

JGR

Journal of Geophysical Research: Space Physics

RESEARCH ARTICLE
10.1002/2014JA020731

Key Points:
- Ionospheric scintillation
- Lunar tide effects over scintillation
- Vertical plasma drift and thermospheric wind

Correspondence to:
E. R. de Paula,
eurico@dae.inpe.br

Citation:
de Paula, E. R., O. F. Jonah, A. O. Moraes, E. A. Kherani, B. G. Fejer, M. A. Abdu, M. T. A. H. Muella, I. S. Batista, S. L. G. Dutra, and R. R. Paes (2015), Low-latitude scintillation weakening during sudden stratospheric warming events, *J. Geophys. Res. Space Physics*, *120*, 2212–2221, doi:10.1002/2014JA020731.

Received 13 OCT 2014
Accepted 10 FEB 2015
Accepted article online 12 FEB 2015
Published online 16 MAR 2015

Low-latitude scintillation weakening during sudden stratospheric warming events

E. R. de Paula[1], O. F. Jonah[1], A. O. Moraes[2], E. A. Kherani[1], B. G. Fejer[3], M. A. Abdu[1], M. T. A. H. Muella[4], I. S. Batista[1], S. L. G. Dutra[1], and R. R. Paes[1]

[1]National Institute for Space Research, São Paulo, Brazil, [2]Aeronautics and Space Institute, São Paulo, Brazil, [3]Atmospheric and Space Sciences, Utah State University, Logan, Utah, USA, [4]Instituto de Pesquisa e Desenvolvimento, Universidade do Vale do Paraiba, São Paulo, Brazil

Abstract Global Positioning System (GPS) L1-frequency (1.575 GHz) amplitude scintillations at São José dos Campos (23.1°S, 45.8°W, dip latitude 17.3°S), located under the southern crest of the equatorial ionization anomaly, are analyzed during the Northern Hemisphere winter sudden stratospheric warming (SSW) events of 2001/2002, 2002/2003, and 2012/2013. The events occurred during a period when moderate to strong scintillations are normally observed in the Brazilian longitude sector. The selected SSW events were of moderate and major categories and under low *Kp* conditions. The most important result of the current study is the long-lasting (many weeks) weakening of scintillation amplitudes at this low-latitude station, compared to their pre-SSW periods. Ionosonde-derived evening vertical plasma drifts and meridional neutral wind effects inferred from total electron content measurements are consistent with the observed weakening of GPS scintillations during these SSW events. This work provides strong evidence of SSW effects on ionospheric scintillations and the potential consequences of such SSW events on Global Navigation Satellite System-based applications.

1. Introduction

The generation of premidnight equatorial ionospheric irregularities or plasma bubbles is determined by sunset electrodynamic processes resulting mainly from eastward thermospheric wind-driven enhanced prereversal upward plasma drifts and upward propagating lower atmospheric waves. The complex set of processes involved in the bubble irregularity phenomenon is also affected by the flux tube integrated Pedersen conductivity, the magnetic field line integrated density, and the longitudinal conductivity gradient across the sunset terminator [*Abdu*, 2005; *Abdu et al*., 2014; *Fejer et al*., 1999]. Plasma density irregularities with scale sizes of hundreds of meters, associated with larger structures (plasma bubbles), cause scattering and diffraction of radio waves crossing unstable ionospheric regions and can produce large-amplitude and/or phase scintillations on received signals [*Yeh and Liu*, 1982]. The fades on the GPS signals due to scintillations caused by irregularities with scale sizes of about 400 m can be deep and long enough to cause loss of the receiver lock, thus affecting the positional and navigational accuracy. Therefore, a statistical characterization of scintillation patterns can help improve the robustness of Global Navigation Satellite Systems (GNSS) receivers [*Kintner et al*., 2001, 2007; *Carrano and Groves*, 2010; *Moraes et al*., 2011, 2014a, 2014b].

Equatorial and low-latitude ionospheric scintillations exhibit large variability with local time, day-to-day, season, latitude, longitude, and solar and magnetic activities, which makes it difficult to establish their morphology and, consequently, to make accurate predictions of their occurrence. *de Paula et al*. [2007] used GPS data from September 1997 to June 2002 from one array of eight sites to describe, for the first time, the morphology of GPS scintillations over the Brazilian sector. This study showed that these scintillations occur predominantly from September to March and have highest occurrence during December solstice of high solar activity. *Muella et al*. [2013] determined the spatial distribution of GPS scintillations between the crests of the equatorial ionization anomaly (EIA) over Brazil. They reported that there is higher scintillation occurrence in the inner region of the southern crests than in the inner region of the northern crest during both December solstice and equinox seasons, as a result of higher ambient ionization and sharper plasma density gradients. *Muella et al*. [2014] determined the climatology of GPS scintillations close to the magnetic equator over Brazil from solar minimum to solar maximum. They pointed out that the evening and early night ionization trough near the magnetic equator leads to small plasma densities and, therefore, limits the

equatorial scintillations to weak intensity levels. Intensive climatological studies on plasma irregularities have been also done using satellite data [e.g., *Stolle et al*., 2008; *Xiong et al*., 2010, and references therein].

The sudden stratospheric warming (SSW) is a large meteorological fluctuation in the polar stratosphere where over a period of several days the temperature increases substantially and the eastward winds become weaker or reverse to westward. According to *Matsuno* [1971], planetary wave activity in the atmosphere is the main mechanism that may trigger a SSW event. A possible explanation for the phenomenon is based in the preconditioning of the vortex, which happens when the stratospheric zonal flow is displaced into the pole. This preconditioning allows the upward propagating planetary waves to interact with the zonal flow, through wave forcing, which tends to exert significant influence on the stratospheric circulation. This interaction imparts a sudden collapse of the zonal flow, then contributing for the displacement of the stratospheric vortex off the pole and, consequently, to the rise of the stratospheric temperature [*Limpasuvan et al*., 2004]. SSW events also trigger or influence a variety of waves, including tides and gravity waves, which in turn can significantly modify the dynamics of the global lower and upper atmosphere and ionosphere. According to the World Meteorological Organization, a major warming occurs when, at 60° latitude and at 10 hPa (~32 km), the vortex wind reverts from eastward to westward and a stratospheric temperature variation of at least $\Delta T \geq 25$ K is attained.

In the low-latitude and equatorial ionosphere, SSW effects are associated with large semidiurnal perturbations in the dynamo zonal electric fields and vertical plasma drifts [e.g., *Chau et al*., 2009, 2010; *Fejer et al*., 2010, 2011; *Rodrigues et al*., 2011; *Park et al*., 2012] and in the latitudinal distribution of the ionospheric plasma, including the EIA [*Goncharenko et al*., 2010a, 2010b, 2013]. The semidiurnal lunar tidal effects on the vertical plasma drifts over Jicamarca were discussed by *Fejer et al*. [2010], who found stronger moon effects about 6 days after the new or full moon days. *Fejer et al*. [2011] and *Fejer and Tracy* [2013] pointed out that lunar semidiurnal tidal effects are strongly enhanced during SSW periods. *Pedatella and Liu* [2013], using simulations, showed that the lunar tidal (M_2) effect over the vertical plasma drift variability is about 25% to 30% during SSW. They also pointed out that this lunar influence depends upon the phase of the moon relative to the timing of the SSW. *Chau et al*. [2012] and *Fejer et al*. [2010] using Jicamarca radar data, and *Rodrigues et al*. [2011] using C/NOFS satellite data, observed large morning upward and afternoon downward drifts during SSW events, which was supported by the numerical modeling of *Pedatella and Liu* [2013]. Similar behavior was observed at the 60° magnetic longitude sector over Brazil by *Jonah et al*. [2014]. In that study the daytime vertical plasma drift was inferred from a pair of magnetometers, one located under the magnetic equator and another at an off-equatorial position. More recently, by using ΔTEC (total electron content) parameter, *Paes et al*. [2014] investigated the EIA relative intensity over Brazil during four events of boreal SSW and also reported TEC semidiurnal patterns as consequence of the ionospheric electric field modulation. *Paes et al*. [2014] also observed the intensification (suppression) of the EIA during the morning (afternoon) hours, which causes anomalous distribution of the ionospheric ionization and, consequently, affects the ionospheric scintillation activity. We note that the magnetic field aligned plasma transport driven by transequatorial/meridional neutral winds also contributes to north-south asymmetries in the plasma density distribution of the EIA, which in turn affect the flux tube integrated conductivities and, consequently, may suppress the generation of plasma irregularities and their associated scintillations [*Devasia et al*., 2002; *Abdu et al*., 2006, 2014; *Muella et al*., 2010].

In the present paper we report long-lasting weakening in the scintillation activity and intensity observed at one GPS station located near the southern crest of the EIA, during the 2001/2002, 2002/2003, and 2012/2013 SSW events. We also examine the possible roles of the equatorial vertical plasma drifts and thermospheric neutral winds on the L band scintillation activity during these events.

2. Data and Results

In this work we use the S_4 scintillation index [*Beach and Kintner*, 2001] to quantify the fluctuations in the amplitude of the GPS signals. The S_4 index was calculated as the standard deviation of the signal intensity relative to its average computed every minute from 18 to 06 LT. High data sampling (50 Hz) scintillation monitor installed at the low-latitude station of São José dos Campos (23.1°S, 45.8°W, dip latitude 17.3°S) was used in the analysis. The S_4 measurements from a nearby station, Cachoeira Paulista (22.4°S, 45°W, dip latitude 16.9°S), have also been used to complement few days of missing data at São José dos Campos. The

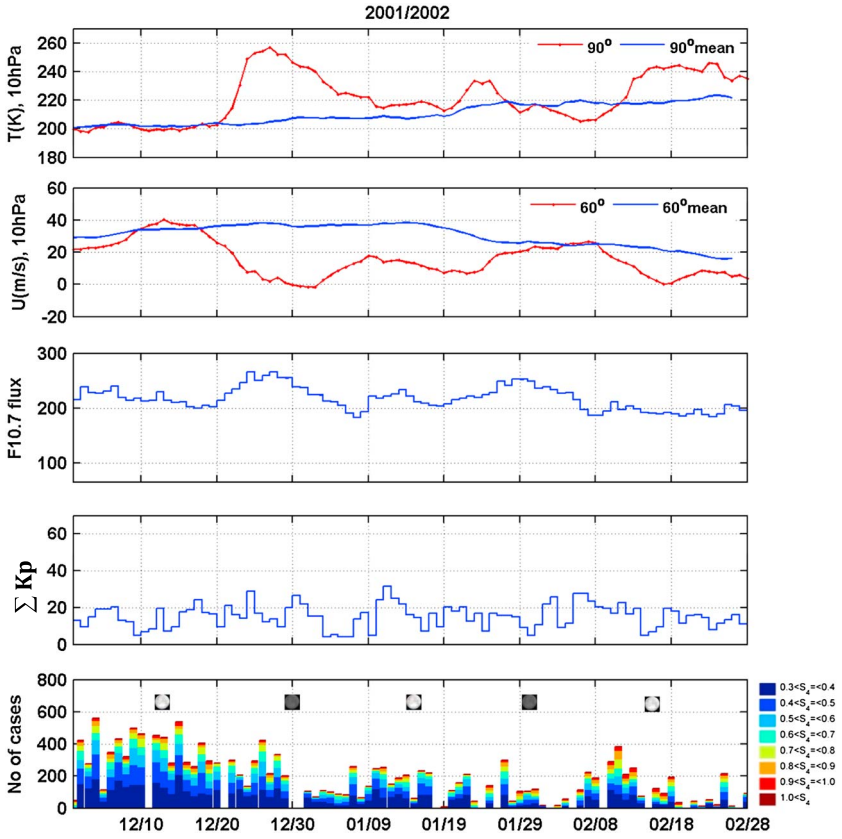

Figure 1. Stratospheric temperature at 90°N, average zonal wind at 60°N and at 32 km of altitude (red lines), $F_{10.7}$ cm solar flux, daily $\sum Kp$, and S_4 scintillation indices for the SSW event of 2001/2002 (December to February). The blue lines in the first and second panels indicate historical average of stratospheric parameters. The different S_4 amplitudes are color coded and represented at the right side of the plot.

first step of this work was to analyze the São José dos Campos ionospheric scintillation data during the Northern Hemisphere SSW events covering the period of 2001 to 2014 and select the periods during magnetic quiet conditions. These warming events occurred during the periods of December to February 2001/2002 (average $F_{10.7} = 209.55$ solar flux unit (sfu)), 2002/2003 (average $F_{10.7} = 137.40$ sfu), and 2012/2013 (average $F_{10.7} = 113.40$ sfu). The first two events occurred around the maximum of the solar cycle 23 and the later around the maximum of the solar cycle 24. Except during solar minimum periods, moderate to high scintillation levels are generally observed around the EIA in the Brazilian sector from December to February [*de Paula et al.*, 2007].

Figure 1 presents the stratospheric, solar, geomagnetic conditions, and the S_4 indices registered during the SSW event of 2001/2002. The stratospheric data were collected from the National Center for Environmental Prediction (http://www.ncep.noaa.gov/). The first and second panels show in red lines the polar stratospheric temperatures at 90°N and zonal average winds at 60°N at geopotential height of 10 hPa (~32 km) and in blue lines their historical averages from the last 30 years. In this event, the eastward winds first weakened and then reversed to westward, which is an indicative of a major warming event. The third and fourth panels present, respectively, the $F_{10.7}$ cm solar indices and the daily $\sum Kp$ indices. The solar flux data were collected from the Space Physics Data Facility provided by NASA at http://omniweb.gsfc.nasa.gov/ website. The geomagnetic planetary *Kp* data were collected from the World Data Center for Geomagnetism at http://wdc.kugi.kyoto-u.ac.jp/ website. The fifth panel presents the number of cases of different S_4 amplitudes specified by colors, from 19 to 24 LT for all available GPS satellites. Only cases with S_4 index larger or equal to 0.3 were considered in the analysis. In order to investigate the possible influence of the lunar gravitational factor, the shaded and unshaded circles also indicated in the S_4 fifth panel denote, respectively, the days of new (shaded circles) and full (unshaded circles) moon phases. Figure 1 shows the occurrence of strong scintillation

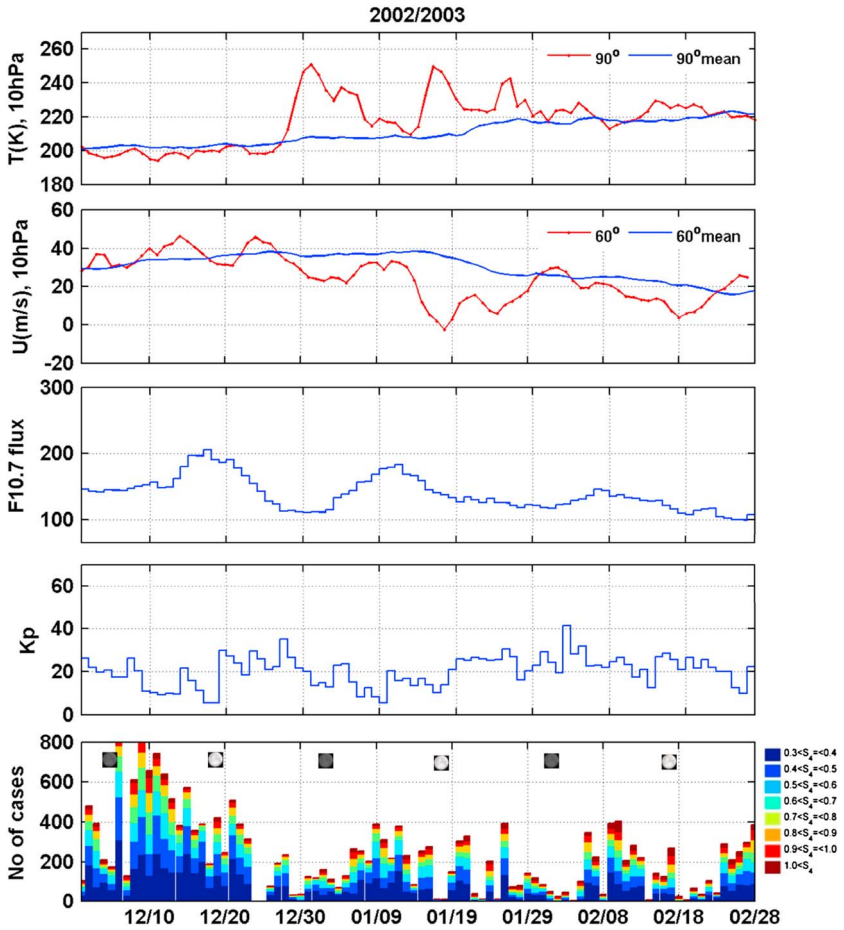

Figure 2. The same as in Figure 1 but for the 2002/2003 SSW event.

activity up to about 20 December, when the arctic temperature began to increase and simultaneously the zonal average wind eastward velocity at 60°N around 32 km height began to decrease. With the onset of the SSW, a long period of weakening in the S_4 amplitude scintillation index, delayed from 20 December to 30 December probably due to the simultaneous solar activity increase, was observed which lasted up to the end of January 2002. Later, the scintillation activity intensified again concurrently with the recovery of the stratospheric temperature and wind to their historical averages. Small stratospheric temperature increase and eastward wind decrease were observed also after 8 February 2002, which appears to have caused another weakening in the S_4 index after 18 February 2002.

Figure 2 presents measurements of stratospheric temperatures and winds, solar flux, geomagnetic, and S_4 indices prior to and during the 2002/2003 SSW event, which occurred in the beginning of solar cycle 23. This figure shows again long-lasting weak S_4 activity starting at about the SSW onset on 28 December and lasting up to about the end of February. In this event there were three stratospheric temperature peaks and small increases up to 20 February, relative to its historical average. Also in this period, the decrease of the eastward wind was recurrent and lasted up to 23 February, and probably, these two effects caused the long S_4 weakening.

The 2012/2013 SSW event occurred under very quiet magnetic conditions, as shown in Figure 3. Again, the results demonstrate the weakening in the scintillation intensity as observed from the S_4 values. In this case the long-lasting S_4 weakening was expected to start after 5 January 2013, when the stratospheric temperature increased and the zonal wind became more westward. However, an increase in $F_{10.7}$ index that occurred in the period of 1–19 January caused an increase on S_4 scintillation index so that the SSW-related weakening in the S_4 index prevailed only after 19 January. Weak S_4 indices lasted up to the end of February 2013, even though the temperature has recovered to its historical value on 25 January 2013 and remained with

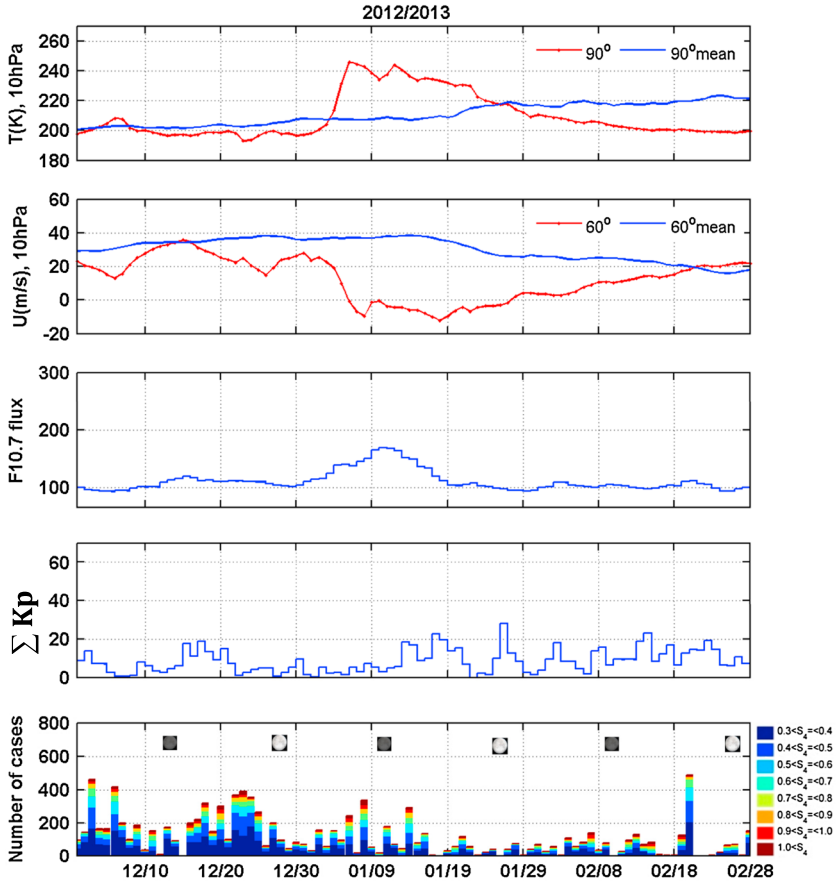

Figure 3. The same as in Figure 1 but for the 2012/2013 SSW event.

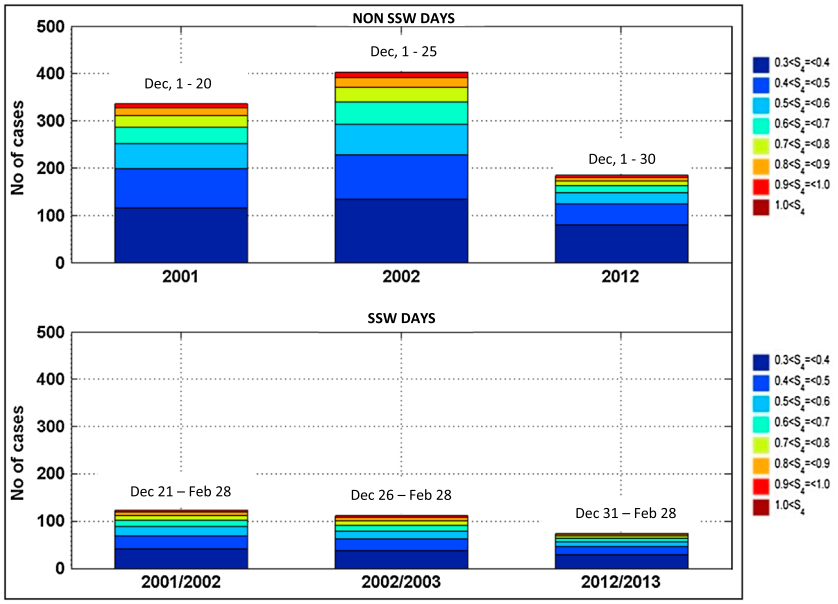

Figure 4. Average number of S_4 cases during the (top) non-SSW days and (bottom) SSW days.

smaller values after that. The wind recovered to its historical value on 20 February 2013, and this long-lasting SSW-disturbed winds might have contributed to this long period of weak scintillations. *Goncharenko et al.* [2013] pointed out that during this 2012/2013 SSW event the associated ionospheric anomalies were observed for over 40 days.

Figure 4 presents the average number of cases for each S_4 amplitude (see the color coded S_4 to the right) during the non-SSW days (top) and during the SSW days of the years of 2001/2002, 2002/2003, and 2012/2013 (bottom). The large S_4 occurrence for these non-SSW days is typical during the December solstice at Brazilian longitudes [*de Paula et al.*, 2007] mainly due to the large vertical plasma drifts during this season. Also at this period, large background ionization contributes to large scintillation amplitude. *Stolle et al.* [2008] and *Abdu et al.* [1998] also observed a larger occurrence of spread *F* (scintillation is normally associated with SF) during December solstice at the Brazilian sector. Figure 4 shows a substantial decrease in the S_4 average number of cases during the SSW days compared to the non-SSW days for the three events. Note that in this figure the number of non-SSW days is much smaller than that of the SSW days.

3. Discussions

We have seen that following the onset of three SSW events, the S_4 scintillation indices exhibited clear long-lasting weakening compared to their pre-SSW values, even though these events occurred during December solstice periods which are normally characterized by high incidence of ionospheric scintillation in the Brazilian sector. The weakening of S_4 scintillation is also evident in SSW months of January and February of 1999, 2000, 2001, and 2002, as shown in the Figure 2 of *de Paula et al.* [2007], but this was not pointed out in that paper since SSW effects on the equatorial ionosphere were not known at that time.

The three important factors that control the plasma bubble development [*Abdu*, 2005; *Abdu et al.*, 2014] and, consequently, ionospheric scintillations are the following: (a) the variability in the growth rate of the instability process owing to the evening vertical plasma drifts, (b) the flux tube integrated conductivity subject to modification by thermospheric meridional winds, and (c) wave modulations of the *F* layer bottomside caused by atmospheric waves (normally gravity waves) traveling upward to serve as seeding source. In addition, the background plasma density also affects the amplitude of the S_4 scintillations.

The evening prereversal enhancement in the vertical drift (PRE vertical drift) is one of the most important parameter controlling the irregularity generation [*Fejer et al.*, 1999]. We have used digital ionosonde data from the equatorial site of São Luís (2.52°S, 44.3°W, dip latitude 1.73°S) to calculate the vertical drifts at 15 min cadence during the time interval from 17 to 20 LT prior and during the SSW periods discussed above. The vertical drifts were calculated by the time rate of change of the true height at 7 MHz. Figure 5 shows the estimated vertical plasma drift velocities during selected SSW days after the stratospheric temperature peaks that are identified by the color legends shown at the right side of the panels. The averaged vertical drift velocities of the 6 days prior to the SSW events, corresponding to the same moon phase of the SSW days, are shown in the panels as reference curves (black thick lines with standard deviation bars). The days used in the average drifts calculation are 20–26 December 2001, 11–17 December 2002, and 17–23 December 2012. It should be pointed out that the prereversal vertical drift velocity just prior to its peak amplitude that usually occurs during 1800–1840 LT (as can be verified from the black curves in Figure 5) is a fundamentally important parameter for the postsunset development of plasma bubble irregularities that produce scintillations. The plots in Figures 5a–5c show that the equatorial vertical plasma drifts decreased on the SSW days during all the three events when compared to the mean values of vertical drifts observed during the days that preceded the events. The results from all the three cases of the SSW events discussed here may suggest that the vertical drift is at least partially responsible for the weakening of the scintillation. However, the observed magnitudes of the vertical drift velocities during the SSW periods alone may not be sufficient to fully explain the weakening in the scintillations. Since the evening thermospheric zonal wind plays a fundamentally important role in the development of the PRE vertical drift [*Rishbeth*, 1971], a decrease in such wind could be occurring during the SSW activity. This may be associated with an increase in the meridional wind that can cause an additional suppression in the bubble irregularity development and hence in S_4 index.

A thermospheric meridional/transequatorial wind can enhance the field line integrated conductivity of an unstable flux tube leading to suppression of the plasma bubble instability growth [see, e.g., *Maruyama*, 1988;

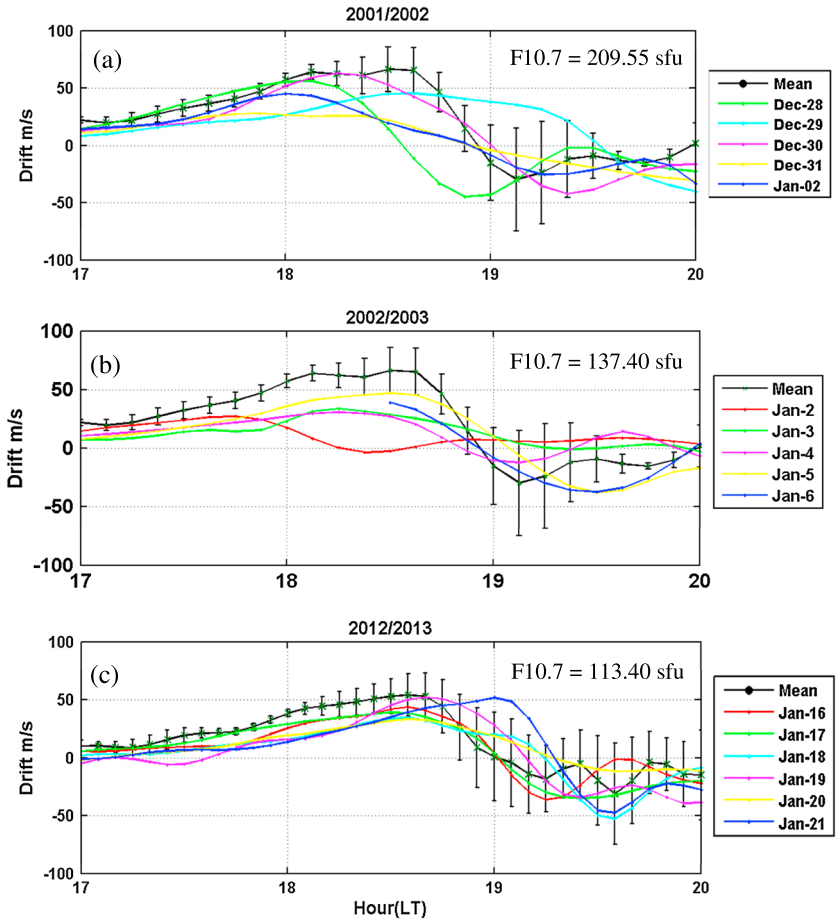

Figure 5. Equatorial vertical plasma drifts for some selected SSW days (colored lines) and for the average of six pre-SSW days (black line) corresponding to the same moon phase of the SSW days and the standard deviation, inferred from the São Luís digital ionosonde data. Average $F_{10.7}$ for the December to February periods are also shown.

Abdu et al., 2014] and hence cause decrease or nonoccurrence of the scintillation. It can also cause latitudinal asymmetry in the EIA crests. According to the simulations of *Pedatella and Liu* [2013], during SSW events, the migrating semidiurnal solar SW2 tide gives rise to neutral temperature increases in the Northern Hemisphere at altitudes of about 130 km. These semidiurnal temperature increases, and the resulting equatorward gradients [*Laskar and Pallamraju*, 2014], drive equatorward meridional winds during SSW events at postsunset hours. Since we do not have wind measurements during our events, we used measurements of the latitudinal distribution of the TEC during 18–20 LT in an attempt to infer any meridional wind effects prior to and during the 2012/2013 SSW. This event was the only one selected here, since the number and distribution of the GNSS receivers available in Brazil before 2007 did not produce reliable TEC maps for the other events.

Figure 6 shows the ΔTEC for the magnetic longitude of 60°W for dip latitudes from 20°S to 20°N before and during the 2012/2013 event and also the Northern Hemisphere stratospheric temperatures and their historical averages. The absolute TEC maps and the ΔTEC contours were obtained using the Nagoya model [*Otsuka et al.*, 2002] and measurements from the International GNSS Service (IGS) and Brazilian Network for Continuous Monitoring (RBMC/IBGE) stations (http://www.ibge.gov.br/home/geociencias/). The $\Delta TEC = TEC - TEC_{av}$ was calculated, where TEC is the absolute total electron content measured in total electron content unit (TECU) (1 TECU = 10^{16} el/m^2) and TEC_{av} is its values averaged in the 18–20 LT interval during each lunar phase from December 2012 to February 2013 [*Jonah et al.*, 2014].

Figure 6 shows a significant degree of asymmetry in the EIA TEC (larger intensity of the southern crest) especially from December 2012 till around 19 January 2013. As may be noted in the figure the EIA crest in TEC

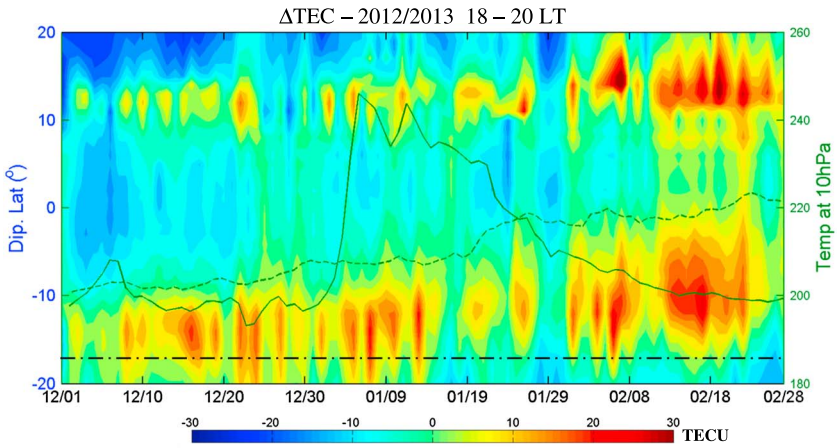

Figure 6. ΔTEC latitudinal distribution at 60°W from 18 to 20 LT around the 2012/2013 SSW event. The continuous line represents the stratospheric temperature for this period, and the dashed line represents the historical stratospheric temperature average. The dash-dotted line represents dip latitude (17.3°S) of São José dos Campos.

is displaced equatorward by a few degrees from the N_mF_2 crest that is nominally located at ±15–18° and commonly referred to as the EIA crest [*Nogueira et al*., 2013]. In this paper we are assuming that the TEC crest represents to some degree the EIA crest since we do not have measurements of the N_mF_2 latitudinal distribution. The asymmetric distribution of the TEC in this case is in part due to larger ionization production by the more intense solar radiation around the subsolar point located in the southern summer hemisphere and also by northward thermospheric winds in the evening hours uplifting the ionospheric plasma to higher altitudes where the recombination rate is smaller, maintaining a larger ionization density in the southern EIA crest (contributing to more intense EIA asymmetry). Such EIA asymmetry does not seem to be a significant factor in the weakening of the scintillation, since the S_4 index was strong enough (as typical of its seasonal behavior) till the onset of the SSW. With the SSW onset on 4 January we note an unexpected increase in the TEC asymmetry with increase also in S_4 index during 5–15 January, which may be attributed to the significant enhancement in the solar flux that occurred during this period (see Figure 3 (third panel)). The period from 15 January to the end of warming is marked by a remarkable degree of symmetry in the TEC latitudinal distribution. This must be the result of a competing influence of the background wind that is dominantly northward during this period and a southward wind originating from the SSW processes (mentioned above). Such a situation may lead to the decrease of the scintillation as compared to its pre-SSW value (characterized as being strong scintillation) that occurred in the presence of an EIA asymmetry and a northward wind. In other words, if the presence of a finite field line integrated conductivity, which influences negatively the nonlinear growth of the bubble instability, permits intense scintillation to occur in the presence of a northward wind, the weakening/reversal of such a wind by an opposing wind due to the SSW should be able to cause enhancement in the field line integrated conductivity leading to S_4 decrease. This reasoning is based on the fact that the field line integrated conductivity existing in an asymmetric EIA produced solely from an asymmetric ionization production (without any meridional wind) has significantly larger contribution to it from the hemisphere of enhanced ionization production, which is the Southern Hemisphere in our case. A northward wind that lifts up the ionization in the Southern Hemisphere can cause decrease in the integrated conductivity of the southern sector more than it can increase it in the northern sector, thereby causing a decrease of the total field line integrated conductivity with respect the nonwind condition. This situation characterized the pre-SSW scintillation. With the SSW in progress the associated enhanced southward wind appears to have annulled or even reversed to southward the seasonal northward wind causing a significant increase in the total field line integrated conductivity, at the same time causing a more symmetric TEC latitudinal distribution as seen during the period of 15 January to the end of the warming in Figure 6. This result thus suggests that besides the SSW-related modifications on the evening vertical plasma drifts, the existing SSW-induced wind is possibly also playing a role in reducing the scintillation activity.

We may further note that the period that followed the end of the SSW is also marked by the weakest of scintillation intensity as part of an extended duration of such weaker scintillation (as can be noted in Figure 3).

This continuing weak scintillation appears to be part of the seasonal trend in the scintillation activity characterized by a slow, but steady, decrease in activity from its December maximum toward its winter minimum to occur in the months of June. According to *Abdu et al*. [1992], over Cachoeira Paulista (very close to São José dos Campos) and from 1980 to 1981, the spread *F* (SF) percentage was about 90% during December and decreased to about 60%–70% during February (SF and scintillation are closely related). So the seasonal scintillation behavior that is a decrease of occurrence from December to February should also be considered as a contributing factor to the S_4 long-lasting weakening observed at all three SSW events. Another important aspect observed in Figure 6 is that the southern EIA peaks tend to displace toward the magnetic equator during the SSW event period, and this fact may also explain in part the weakening of the scintillation, since the background plasma density at the dip latitude of São José dos Campos (as indicated by the dash-dotted line in Figure 6) is significantly reduced. This later effect on the day-to-day variability of plasma irregularities/scintillations during SSW events is going to be further investigated.

Similar studies should be carried out during other SSW periods and also in other sectors where meridional wind and vertical drifts effects might be somewhat different.

4. Conclusions

On the basis of the above discussion we may conclude that the role of both vertical plasma drift and thermospheric meridional wind, which are significantly modified during the three SSW events analyzed in this study, is responsible for the weakening of the scintillation.

The main conclusions of this study may be summarized as follows:

1. The scintillation intensity (represented by the S_4 index) over a station under the southern crest of the EIA in the American sector can be weakened significantly during SSW events. The weakening effect is found to be long lasting (many weeks) and was consistently observed during the SSW events of 2001/2002, 2002/2003, and 2012/2013.
2. The vertical drift velocity, around the prereversal peak hour, was consistently smaller during all the SSW days as compared to the pre-SSW days.
3. The latitudinal symmetry of the EIA as observed in the ΔTEC during the 2012/2013 SSW event suggested a meridional/equatorward thermospheric wind induced by stratospheric warming in the Northern Hemisphere, together with the weakening of vertical drift, as another factor that contributed to the scintillation weakening during that event.
4. One interesting characteristic observed in Figure 6 throughout the 2012/2013 SSW event was the displacement of the southern crest of the EIA to latitudes closer to the magnetic dip equator, occasioning a reduction in the background ionization above the low-latitude station of São José dos Campos and, consequently, contributing also to the decline in the scintillation intensity at the site.
5. The seasonal scintillation behavior over the Brazilian sector, which is a decrease of occurrence from December to February, should also be considered as a contributing factor to the S_4 long-lasting weakening observed at all three SSW events.
6. The events analyzed in this study provided strong evidences of SSW effects on the seasonal (southern summer solstice) variability of ionospheric irregularities at low latitudes, contributing to the establishment of GNSS scintillation pattern during such type of events, which is a relevant theme for the scientific and technical community involved in the scintillation prediction.

Acknowledgments

Stratospheric, geomagnetic, and solar flux data were collected from the National Centers for Environmental Prediction, from http://wdc.kugi.kyoto-u.ac.jp/ website and from http://omniweb.gsfc.nasa.gov/form/dx1 website, respectively. TEC data were collected from the International GNSS Service (IGS) and Brazilian Network for Continuous Monitoring (RBMC/IBGE) stations (http://www.ibge.gov.br/home/geociencias/). E.R. de Paula is grateful to AFOSR FA9550-10-1-0564 and Conselho Nacional de Desenvolvimento Científico e Tecnológico (CNPq) 305684/2010-8 grants. M.A. Abdu, A.O. Moraes, O.F. Jonah, and M.T.A.H. Muella would also like to thank the support from CNPq under processes 300883/2008-0, 5360301/2010- O, 133429/2011-3, and 308017/2011-0, respectively. E.A. Kherani is grateful to FAPESP under process 2011/21903-3.

Alan Rodger thanks Anthea Coster and another reviewer for their assistance in evaluating this paper.

References

Abdu, M. A. (2005), Equatorial ionosphere-thermosphere system: Electrodynamics and irregularities, *Adv. Space Res.*, *35*, 771–787, doi:10.1026/j.asr.2005.03.150.

Abdu, M. A., I. S. Batista, and J. H. A. Sobral (1992), A new aspect of magnetic declination control of equatorial spread F and F region dynamo, *J. Geophys. Res.*, *97*(A10), 14,897–14,904, doi:10.1029/92JA00826.

Abdu, M. A., J. H. A. Sobral, I. S. Batista, V. H. Rios, and C. Medina (1998), Equatorial spread-F occurrence statistics in the American longitudes: Diurnal, seasonal and solar cycle variations, *Adv. Space Res.*, *22*(6), 851–854.

Abdu, M. A., K. N. Iyer, R. T. de Medeiros, I. S. Batista, and J. H. A. Sobral (2006), Thermospheric meridional wind control of equatorial spread F and evening prereversal electric field, *Geophys. Res. Lett.*, *33*, L07106, doi:10.1029/2005GL024835.

Abdu, M. A., E. A. Kherani, I. S. Batista, B. W. Reinish, and J. H. A. Sobral (2014), Equatorial spread *F* initiation and growth from satellite traces as revealed from conjugate point observations in Brazil, *J. Geophys. Res. Space Physics*, *119*, 1–9, doi:10.1002/2013JA019352.

Beach, T. L., and P. M. Kintner (2001), Development and use of a GPS ionospheric scintillation monitor, *IEEE Trans. Geosci. Remote Sens.*, *39*, 918–928.

Carrano, C. S., and K. M. Groves (2010), Temporal decorrelation of GPS satellite signals due to multiple scattering from ionospheric irregularities, in *Proceedings of the ION-GNSS-10*, pp. 361–374, Institute of Navigation, Portland, Ore.

Chau, J. L., B. G. Fejer, and L. P. Goncharenko (2009), Quiet variability of equatorial E × B drifts during a sudden stratospheric warming event, *Geophys. Res. Lett.*, *36*, L05101, doi:10.1029/2008GL036785.

Chau, J. L., N. A. Aponte, E. Cabassa, M. P. Sulzer, L. P. Goncharenko, and S. A. Gonzalez (2010), Quiet time ionospheric variability over Arecibo during sudden stratospheric warming events, *J. Geophys. Res.*, *115*, A00G06, doi:10.1029/2010JA015378.

Chau, J. L., L. P. Goncharenko, B. G. Fejer, and H. Liu (2012), Equatorial and low latitude ionospheric effects during sudden stratospheric warming events, *Space Sci. Rev.*, *168*(1–4), 385–417, doi:10.1007/s11214-011-9797-5.

de Paula, E. R., et al. (2007), Characteristics of the ionospheric irregularities over Brazilian longitudinal sector, *Indian J. Radio Space Phys.*, *36*, 268–277.

Devasia, C. V., N. Jyoti, K. S. V. Subbarao, K. S. Viswanathan, D. Tiwari, and R. Sridharan (2002), On the plausible linkage of thermospheric meridional winds with the equatorial spread *F*, *J. Atmos. Sol. Terr. Phys.*, *64*, 1–12.

Fejer, B. G., and B. D. Tracy (2013), Lunar tidal effects in the electrodynamics of the low latitude ionosphere, *J. Atmos. Sol. Terr. Phys.*, *103*, 76–82.

Fejer, B. G., L. Scherliess, and E. R. de Paula (1999), Effects of the vertical plasma drifts velocity on the generation and evolution of equatorial spread *F*, *J. Geophys. Res.*, *104*, 19,859–19,869, doi:10.1029/1999JA900271.

Fejer, B. G., M. E. Olson, J. L. Chau, C. Stolle, H. Lühr, L. P. Goncharenko, K. Yumoto, and T. Nagatsuma (2010), Lunar-dependent equatorial ionospheric electrodynamic effects during sudden stratospheric warming, *J. Geophys. Res.*, *115*, A00G03, doi:10.1029/2010JA015273.

Fejer, B. G., B. D. Tracy, M. E. Olson, and J. L. Chau (2011), Enhanced lunar semidiurnal equatorial vertical plasma drifts during sudden stratospheric warmings, *Geophys. Res. Lett.*, *38*, L21104, doi:10.1029/2011GL049788.

Goncharenko, L. P., J. L. Chau, H.-L. Liu, and A. J. Coster (2010a), Unexpected connections between stratosphere and ionosphere, *Geophys. Res. Lett.*, *37*, L10101, doi:10.1029/2010GRL043125.

Goncharenko, L. P., A. J. Coster, J. L. Chau, and C. E. Valladares (2010b), Impact of sudden stratospheric warming on equatorial ionization anomaly, *J. Geophys. Res.*, *115*, A00G07, doi:10.1029/2010JA015400.

Goncharenko, L., J. L. Chau, P. Condor, A. J. Coster, and L. Benkevitch (2013), Ionospheric effects of sudden stratospheric warming during moderate-to-high solar activity: Case study of January 2013, *Geophys. Res. Lett.*, *40*, 1–5, doi:10.1002/grl.50980.

Jonah, O. F., E. R. de Paula, E. A. Kherani, S. L. G. Dutra, and R. R. Paes (2014), Atmospheric and ionospheric response to stratospheric sudden warming of January 2013, *J. Geophys. Res. Space Physics*, *119*, 4973–4980, doi:10.1002/2013JA019491.

Kintner, P. M., H. Kil, T. L. Beach, and E. R. de Paula (2001), Fading timescales associated with GPS signal and potential consequences, *Radio Sci.*, *36*, 731–743, doi:10.1109/1999RS002310.

Kintner, P. M., B. M. Ledvina, and E. R. de Paula (2007), Size, shape, orientation, speed, and duration of GPS equatorial anomaly scintillations, *Radio Sci.*, *39*, RS2012, doi:10.1029/2003RS002878.

Laskar, F. I., and D. Pallamraju (2014), Does sudden stratospheric warming induce meridional circulation in the mesosphere thermosphere system?, *J. Geophys. Res. Space Physics*, *119*, 10,133–10,143, doi:10.1002/2014JA020086.

Limpasuvan, V., D. W. J. Thompson, and D. L. Hartmann (2004), The life cycle of the Northern Hemisphere sudden stratospheric warmings, *J. Clim.*, *17*, 2584–2596.

Maruyama, T. (1988), A diagnostic model for equatorial spread *F*: 1. Model description and application to electric fields and neutral winds effects, *J. Geophys. Res.*, *93*, 14,611–14,622, doi:10.1029/JA093iA12p14611.

Matsuno, T. (1971), A dynamical model of the stratospheric sudden warmings, *J. Atmos. Sci.*, *28*, 1479–1494.

Moraes, A. O., F. S. Rodrigues, E. R. de Paula, and W. J. Perrella (2011), Analysis of the characteristics of low-latitude GPS amplitude scintillation measured during solar maximum conditions and implications for receiver performance, *Surv. Geophys.*, *33*(5), doi:10.1007/s10712-011-9161-z.

Moraes, A. O., E. R. de Paula, M. T. A. H. Muella, and W. J. Perrella (2014a), On the second order statistics for GPS ionospheric scintillation modeling, *Radio Sci.*, *49*, doi:10.1002/2013RS005270.

Moraes, A. O., E. Costa, E. R. de Paula, W. J. Perrella, and J. F. G. Monico (2014b), Extended ionospheric amplitude scintillation model for GPS receivers, *Radio Sci.*, *49*, 315–333, doi:10.1002/2013RS005307.

Muella, M. T. A. H., E. R. de Paula, P. R. Fagundes, J. A. Bittencourt, and Y. Sahai (2010), Thermospheric meridional wind control on equatorial scintillations and the role of the evening *F*-region height rise, E × B drift velocities and *F*2-peak density gradients, *Surv. Geophys.*, *31*, 509–530, doi:10.1007/s10712-010-9101-3.

Muella, M. T. A. H., E. R. de Paula, and A. A. Monteiro (2013), Ionospheric scintillation and dynamics of Fresnel-scale irregularities in the inner region of the equatorial ionization anomaly, *Surv. Geophys.*, *34*, 233–251, doi:10.1007/s10712-012-9212-0.

Muella, M. T. A. H., E. R. de Paula, and O. F. Jonah (2014), GPS L1-frequency observations of equatorial scintillations and irregularity zonal velocities, *Surv. Geophys.*, *35*, 335–357, doi:10.1007/s10712-013-9252-0.

Nogueira, P. A. B., M. A. Abdu, J. R. Souza, I. S. Batista, G. J. Bailey, A. M. Santos, and H. Takahashi (2013), Equatorial ionization anomaly development as studied by GPS TEC and foF2 over Brazil: A comparison of observations with model results from SUPIM and IRI-2012, *J. Atmos. Sol. Terr. Phys.*, *104*, 45–54.

Otsuka, Y., T. Ogawa, A. Saito, T. Tsugawa, S. Fukao, and S. A. Miyazaki (2002), New technique for mapping of total electron content using GPS network in Japan, *J. Earth Planets Space*, *54*, 63–70.

Paes, R. R., I. S. Batista, C. M. N. Candido, O. F. Jonah, and P. C. P. Santos (2014), Equatorial ionization anomaly variability over the Brazilian region during boreal sudden stratospheric warming events, *J. Geophys. Res. Space Physics*, *119*, 7649–7664, doi:10.1002/2014JA019968.

Park, J., H. Lühr, M. Kunze, B. G. Fejer, and W. K. Min (2012), Effects of sudden stratospheric warming on lunar tidal modulation of the equatorial electrojet, *J. Geophys. Res.*, *117*, A03306, doi:10.1029/2011JA017351.

Pedatella, N. M., and H. Liu (2013), The influence of atmospheric tide and planetary wave variability during sudden stratosphere warmings on the low latitude ionosphere, *J. Geophys. Res. Space Physics*, *118*, 1–15, doi:10.1002/jgra.50492.

Rishbeth, H. (1971), Polarization fields produced by winds in the equatorial F region, *Planet. Space Sci.*, *19*, 357–369.

Rodrigues, F. S., G. Crowley, S. M. I. Azeem, and R. A. Heelis (2011), C/NOFS observations of the equatorial electric field response to the 2009 major stratospheric warming event, *J. Geophys. Res.*, *116*, A09316, doi:10.1029/2011JA016660.

Stolle, C., H. Lühr, and B. G. Fejer (2008), Relation between the occurrence rate of ESF and the equatorial vertical plasma drift velocity at sunset derived from global observations, *Ann. Geophys.*, *26*, 3979–3988.

Xiong, C., J. Park, H. Lühr, C. Stolle, and S. Y. Ma (2010), Comparing plasma bubble occurrence rates at CHAMP and GRACE altitudes during high and low solar activity, *Ann. Geophys.*, *28*, 1647–1658.

Yeh, K. C., and C. K. Liu (1982), Radio wave scintillations in the ionosphere, *Proc. IEEE*, *70*(4), 324–360, doi:10.1109/PROC.1982.12313.